

ESTIMATION OF WAVE DRIFT FORCE BY NUMERICAL WAVE TANK

Katsuji Tanizawa, Makiko Minami
Ship Research Institute, Tokyo, Japan

Shigeru Naito
Osaka University, Osaka, Japan

ABSTRACT

A fully nonlinear numerical wave tank (NWT) is applied to estimation of the wave drift force acting on two-dimensional fixed and floating bodies. This is a time domain simulation program which solves simultaneous equations of ideal fluid motion and floating body motion. Using this NWT, the diffraction problem and the radiation-diffraction problem of a two-dimensional Lewis form body in regular waves are simulated and the wave drift force is calculated both from transmitted wave and from direct pressure integral on the wetted body surface. To examine the accuracy of NWT, the first harmonic components of simulated hydrodynamic forces, body motions, wave reflection and transmission coefficients and wave drift force are compared with linear theory and experimental data of Nojiri (1975). The first harmonic components of the nonlinear simulation are confirmed to be in good agreement with linear theory.

KEY WORDS : Wave drift force, Numerical wave tank, Fully nonlinear simulation, Fluid-body interaction

INTRODUCTION

Recently, forecasting of the course and speed of drifting wrecked ship is one of the urgent topics. When a ship is in distress in rough seas, the coastal guard has to keep tracking of the ship and send rescue boats in minimum delay. If the location of the ship is lost, accurate forecasting systems are indispensable for rescue team to save the human lives and properties. In particular, in the case of wrecked oil carrier, it will be disaster unless rescued swiftly. As a part of development of the forecasting system, the authors study the wave drift force acting on floating body with arbitrary shape in large amplitude waves. Evaluation of the wave drift force is important also for the power evaluation of towing boats. For this purpose, we should consider the effect of forward velocity on the drift force. If the towed ship is in shallow area, the shape of sea bottom may also affect the drift force.

The wave drift force is not a new topic and its mechanism is well understood from the conservation law of energy and momen-

tum of wave field around a floating body (Maruo 1960). However, to meet the above requirement, we need numerical tools to estimate the effect of various parameters on the wave drift force. The numerical wave tank (NWT) can be a powerful tool. The NWT we have developed is a time domain fully nonlinear simulation program which solves simultaneous equations of ideal fluid motion and floating body motion. This type of NWT is originally developed by Vinje and Brevig(1981). After them, Cointe et al.(1990), Tanizawa(1990,1995,1996), Van Daalen(1993), Sen(1993), Cao et al.(1994), Kashiwagi(1996) and others developed NWTs in the past decade. These NWTs are applied to various problems and their accuracy and applicability are demonstrated. The authors have also shown application of our NWT to various problems like large amplitude floating body motions, large amplitude interaction among floating body, incident wave and internal cargo fluid, parametric roll motions, chaotic roll motions, wave drift damping force, etc.

In the present study, we examine the accuracy of our NWT for evaluation of the wave drift force. In the previous study, one of the authors simulated the motions of a two dimensional floating body in a closed tank and showed simulated results satisfy well the conservation law of mass, momentum and energy. As the next examination, we simulated the diffraction problem and the radiation-diffraction problem of a two dimensional Lewis form body in regular waves and compared the simulated results with the linear theory and experimental data of Nojiri (1975).

OUTLINE OF THE NUMERICAL SIMULATION

Fully Nonlinear Numerical Wave Tank

Fig.1 shows the numerical wave tank used for the simulation. The fluid domain is bounded by free-surfaces S_f , wave making boundary S_w , bottom and rigid wall S_b and floating body surface S_s . Here, the gravitational acceleration g , the fluid density ρ and the length of incident regular wave λ are chosen as units to nondimensionalize the problem. A space-fixed Cartesian coordinate system $o-xz$ is used, with x coincident with the calm free-surface and z positive upward. The fluid is assumed to be homogeneous, incompressible, inviscid and its motion irrotational.

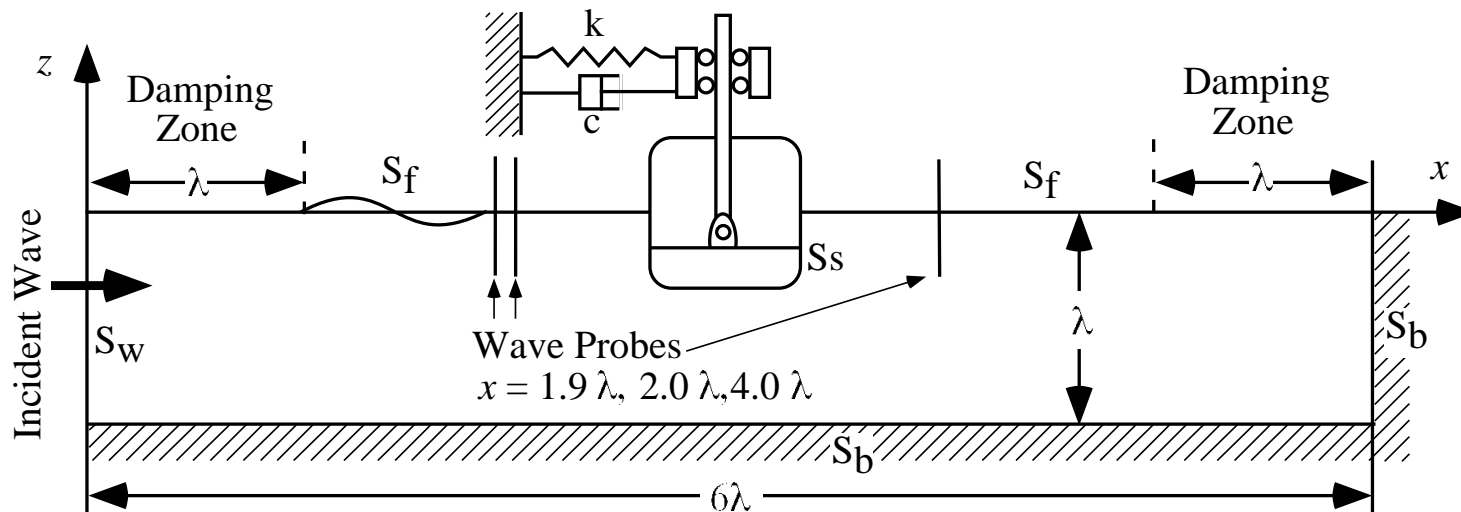


Fig.1: Numerical wave tank

The fluid motion can be described by the velocity potential ϕ and its time derivative ϕ_t . In the fluid domain, ϕ and ϕ_t satisfy Laplace's equation

$$\nabla^2 \phi = \nabla^2 \phi_t = 0. \quad (1)$$

Green's second identity can be applied on both ϕ and ϕ_t

$$c(\mathcal{Q}) \left\{ \begin{array}{l} \phi(\mathcal{Q}) \\ \phi_t(\mathcal{Q}) \end{array} \right\} = \int_S \left\{ \begin{array}{l} \phi(\mathcal{P}) \\ \phi_t(\mathcal{P}) \end{array} \right\} \frac{\partial}{\partial n} \ln r(\mathcal{P}, \mathcal{Q}) \\ - \ln r(\mathcal{P}, \mathcal{Q}) \left\{ \begin{array}{l} \frac{\partial \phi(\mathcal{P})}{\partial n} \\ \frac{\partial \phi_t(\mathcal{P})}{\partial n} \end{array} \right\} dS, \quad (2)$$

where \mathcal{P}, \mathcal{Q} are points on the boundary, n is the outward normal direction of the boundary, $r(\mathcal{P}, \mathcal{Q})$ is the distance between \mathcal{P} and \mathcal{Q} , $c(\mathcal{Q})$ represents the angle subtended at \mathcal{Q} by boundaries.

On the wave making boundary S_w , the flux of linear propagating wave is imposed as the boundary condition.

$$\frac{\partial \phi}{\partial n} = -\frac{k\zeta_A \cosh k(z+h)}{\omega \cosh kh} \cos(kx - \omega t) \quad (3)$$

$$\frac{\partial \phi_t}{\partial n} = -\frac{k\zeta_A \cosh k(z+h)}{\cosh kh} \sin(kx - \omega t) \quad (4)$$

Where k, ω and ζ_A are wave number, angular frequency and wave amplitude of the incident wave, respectively.

On the free-surface, kinematic and dynamic free-surface boundary conditions,

$$\frac{D\phi}{Dt} = -z + \frac{1}{2}(\nabla\phi)^2 - \nu(x_e)(\phi - \phi_e) \quad (5)$$

$$\frac{D\mathbf{x}}{dt} = \nabla\phi - \nu(x_e)(\eta - \eta_e), \quad (6)$$

are imposed, where η is the wave elevation and $\nu(x_e)$ is the damping coefficient

$$\nu(x) = \begin{cases} \alpha\omega\left(\frac{x-x_0}{\lambda}\right)^2, & \text{for } x_0 \leq x \leq x_1 = x_0 + \beta\lambda \\ 0, & \text{for } x < x_0 \text{ or } x > x_1 \end{cases}. \quad (7)$$

The artificial damping terms added to dynamic and kinematic free-surface boundary conditions are effective only inside of damping zones. The performance of this damping zone is controlled by two parameters α and β . α is used to control the strength of

damping and β is used to control the length of damping zone. ϕ_e, η_e are reference values. This damping zone absorbs differences $\phi - \phi_e$ and $\eta - \eta_e$. When the damping zone is placed in front of a rigid wall and works as a simple absorber, the reference values are set to $\phi_e = 0, \eta_e = 0$. On the other hand, when the damping zone is placed in front of a wave making boundary, the reference values are set to

$$\phi_e = \frac{\zeta_A \cosh k(h+z)}{\omega \cosh kh} \sin(kx - \omega t) \quad (8)$$

$$\eta_e = \zeta_A \cos(kx - \omega t) \quad (9)$$

The wave reflection coefficient of this damping zone becomes less than 2%, when the tuning parameters are appropriately set to $\alpha = \beta = 1$ for a regular wave.

On the body surface, impermeability condition with respect to ϕ is expressed as

$$\frac{\partial \phi}{\partial n} = \mathbf{n} \cdot (\mathbf{v}_0 + \boldsymbol{\omega} \times \mathbf{r}), \quad (10)$$

where \mathbf{v}_0 and $\boldsymbol{\omega}$ are translating and angular velocities of the body, respectively.

Impermeability condition on the body with respect to ϕ_t is given as

$$\frac{\partial \phi_t}{\partial n} = -k_n (\nabla\phi - \mathbf{v}_0 - \boldsymbol{\omega} \times \mathbf{r})^2 + \mathbf{n} \cdot (\dot{\mathbf{v}}_0 + \dot{\boldsymbol{\omega}} \times \mathbf{r}) \\ + \mathbf{n} \cdot \boldsymbol{\omega} \times (\boldsymbol{\omega} \times \mathbf{r}) + \mathbf{n} \cdot 2\boldsymbol{\omega} \times (\nabla\phi - \mathbf{v}_0 - \boldsymbol{\omega} \times \mathbf{r}) \\ - \frac{\partial}{\partial n} \left(\frac{1}{2}(\nabla\phi)^2 \right), \quad (11)$$

where k_n is the normal curvature of body surface, $\dot{\mathbf{v}}_0, \dot{\boldsymbol{\omega}}$ are translating and angular accelerations of the body, respectively (Tanizawa, 1995).

On the floating body surface, $\dot{\mathbf{v}}_0$ and $\dot{\boldsymbol{\omega}}$ cannot be specified explicitly. However, using the equation of body motion, $\dot{\mathbf{v}}_0$ and $\dot{\boldsymbol{\omega}}$ can be eliminated and an implicit body surface boundary condition can be derived. Denoting the inertia tensor of a floating body as \mathcal{M} and the generalized normal vector of body surface as $\mathbf{N} = (\mathbf{n}, \mathbf{n} \times \mathbf{r})$, the implicit boundary condition is written as

$$\frac{\partial \phi_t}{\partial n} = \mathbf{N} \mathcal{M}^{-1} \int_{S_s} -\phi_t \mathbf{N} ds \\ + \mathbf{N} \mathcal{M}^{-1} \left\{ \int_{S_s} \left(-z - \frac{1}{2}(\nabla\phi)^2 \right) \mathbf{N} ds + \mathbf{F}_g \right\} \\ + q - \frac{\partial}{\partial n} \left(\frac{1}{2}(\nabla\phi)^2 \right), \quad (12)$$

where \mathbf{F}_g is the sum of gravity, mooring force and other external forces acting to the body and q is the term which can be explicitly evaluated from the solution of the velocity field as

$$q = -k_n (\nabla\phi - \mathbf{v}_o - \boldsymbol{\omega} \times \mathbf{r})^2 + \mathbf{n} \cdot \boldsymbol{\omega} \times (\boldsymbol{\omega} \times \mathbf{r}) + \mathbf{n} \cdot 2\boldsymbol{\omega} \times (\nabla\phi - \mathbf{v}_o - \boldsymbol{\omega} \times \mathbf{r}). \quad (13)$$

With these boundary conditions and Green's second identity with respect to ϕ and ϕ_t , both the velocity and acceleration fields can be solved numerically by means of BEM. The solutions are integrated with respect to time by the 4th order Runge-Kutta method, then the fluid and body motions are simulated in the time domain. The free-surface is traced by the Mixed Eulerian and Lagrangian method (MEL).

Floating Body

Fig.2 and Table 1 show shape and principle dimensions of the Lewis form body used for the simulations. To compare the simulated results with experimental data of Nojiri (1975), we used the same shape and dimensions as his model.

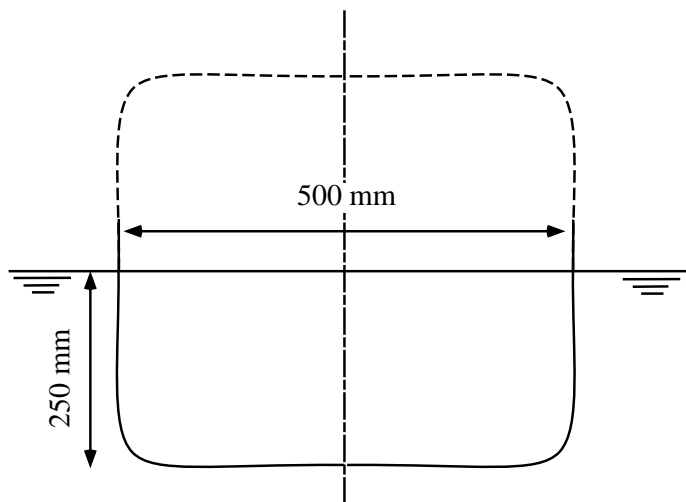


Fig.2 Floating Body

Table 1 Principle Dimensions

Breadth	B	0.50	m
Draft	d	0.25	m
Displacement/Length	W	125.0	kg/m
Lewis Form parameter	H_0	1.00	
	σ	1.00	
Center of inertia	KG	0.135	m
Spring constant	k	197.58	N/m
Damping coefficient	c	19.80	N

Size of numerical wave tank and discretization

As Fig.1 shows, the length and the depth of NWT are 6λ and λ , respectively. Number of collocation points are 10 on both sides of NWT, 40 on the bottom, 120 on the free-surface and 34 on the floating body surface. The time step is set to $1/20$ of the incident wave period T_w .

Incident Waves

Regular waves, with nondimensional wavenumber $\xi_B (= \frac{\omega^2 B}{g})$ ranging from 0.25 to 2.00 and wave height of $H_I = 1cm$ and $7cm$, are used for simulations. Combinations of wave length and wave height are given in Table 2.

Table 2 Incident Waves

ξ_B	$\lambda(m)$	Wave Slope	
		$H_I = 1.0cm$	$H_I = 7.0cm$
0.25	6.283	1/628	1/90
0.50	3.142	1/314	1/45
0.55	2.856	1/286	1/41
0.60	2.618	1/262	1/37
0.65	2.417	1/242	1/35
0.70	2.244	1/224	1/32
0.75	2.094	1/209	1/30
1.00	1.571	1/157	1/22
1.25	1.257	1/126	1/18
1.50	1.047	1/105	1/15
1.75	0.898	1/90	1/13
2.00	0.785	1/79	(1/11)

SIMULATED RESULTS

The diffraction problem of a fixed body and the radiation-diffraction problem of a weakly moored floating body are simulated. Results are presented from Fig.3 to Fig.7 using the following nondimensional values,

Time	; t/T_w
Sway force	; $F_S/\rho g L d \zeta_A$
Heave force	; $F_H/\rho g L B \zeta_A$
Roll moment	; $M_R/\rho g L B d \zeta_A$
Sway amp.	; X_A/ζ_A
Heave amp.	; Z_A/ζ_A
Roll amp.	; $\theta_A/k \zeta_A$
Ref. coef.	; $H_R/H_I (= \zeta_R/\zeta_A)$
Trans. coef.	; $H_T/H_I (= \zeta_T/\zeta_A)$
Drift force	; $F_D/\frac{1}{2}\rho g L \zeta_A^2$

where L is length of the body and $L \equiv 1$ for two dimensional simulations.

Diffraction Problem

Fig.3 shows the simulated time histories of wave exciting forces acting on a fixed body. When the wave height is low, $H_I = 1cm$, simulated wave exciting forces are harmonic and slight distortion in the wave form is observed only on the heave force in short wave $\lambda = 1.047m$. However, when the wave height is high, $H_I = 7cm$, significant higher frequency components are observed in the simulated time history, particularly on the heave force in short waves. Although nonlinear components are interesting, the first harmonic components are the main target of this paper and higher harmonic components are left for future study. Applying the Fourier analysis to the last half of the time histories, $10 < t/T_w \leq 20$, the first harmonic components are obtained.

In Fig.4(a) ~ 4(c), the first harmonic wave exciting forces on the fixed body are plotted using open symbols. The solid line shows the value of linear theory and closed squares show experimental values. We can confirm that the simulated wave exciting forces in

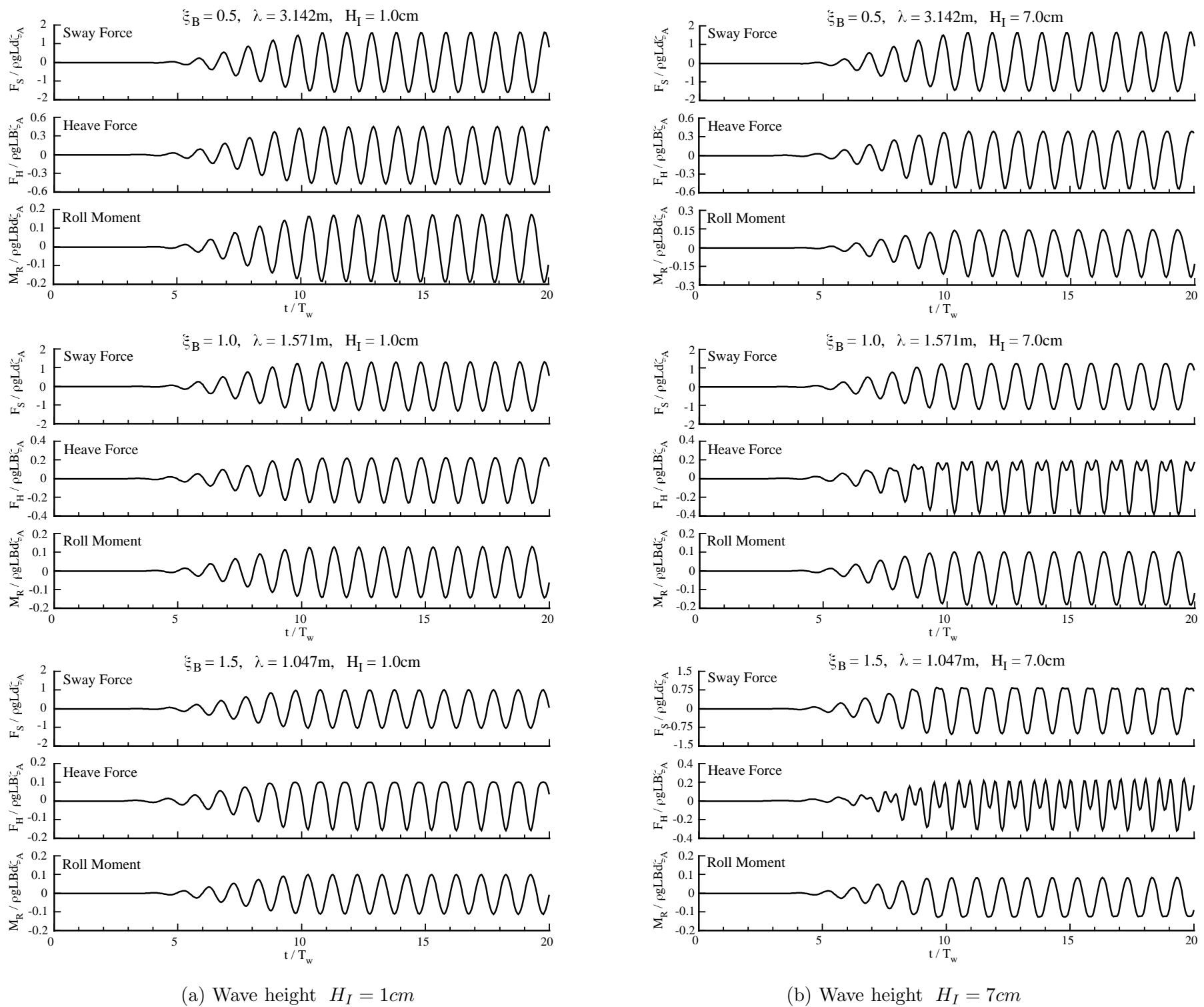


Fig.2: Simulated wave exciting forces on the fixed body

small amplitude waves, $H_I = 1\text{cm}$, agree well with the values of linear theory. As to $H_I = 7\text{cm}$, even though the simulated time histories are distorted from sinusoidal form in the high frequency range, the first harmonic wave exciting forces still agree well with the linear theory and only slight difference can be observed in the high frequency range. The highest frequency for stable simulation is $\xi_B = 1.75$ and the wave slope at this frequency is $1/13$. Even in such a steep wave, the difference between simulated first harmonic wave exciting forces and linear theoretical values are not so significant.

Fig.4(d) and 4(e) show the reflection and transmission coefficients of the incident wave, respectively. The wave reflection coefficient is calculated by Goda's method (1976) using the simulated wave elevation at fixed points $x = 1.9\lambda$ and 2.0λ . The wave transmission coefficient is simply obtained from the simulated wave elevation at fixed point $x = 4.0\lambda$, (see Fig.1). The simulated reflection and transmission coefficients also agree well with the linear

theory except in high frequency range of $H_I = 7\text{cm}$.

Fig.4(f) shows the wave drift force acting on the fixed body. The wave drift force computed from the transmission coefficient agrees well with theoretical value. On the other hand, agreement of the wave drift force by the pressure integral is not good and the value for $H_I = 1\text{cm}$ is worse than that of for $H_I = 7\text{cm}$. The reason of this inaccuracy is not clear now.

Radiation-Diffraction Problem

Fig.5 shows the simulated time history of floating body motions in small $H_I = 1\text{cm}$ and large $H_I = 7\text{cm}$ amplitude waves. In the large amplitude wave, simulated sway motion has long period of oscillation. This long period motion is a transient response of mooring system and its damping is caused by the damping of mooring system (Table 1) and the wave drift damping force (Tanizawa 1997-2). In the large amplitude short wave, the simulated roll

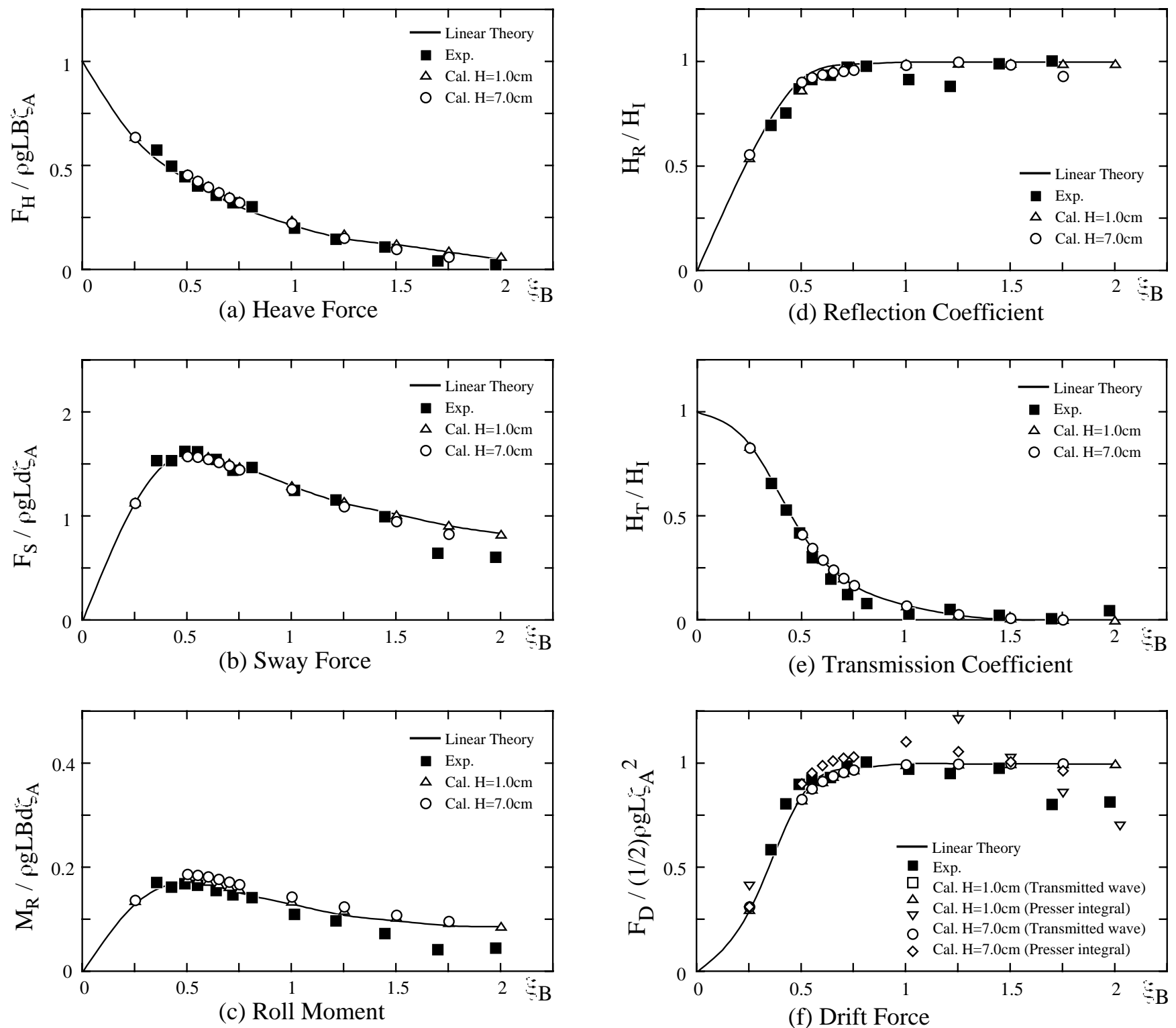


Fig.4: Simulated first harmonic component of the wave exciting forces on the fixed body, wave reflection and transmission coefficients and wave drift force.

motion has constant heeling angle. Such a nonlinear response is also interesting topic. However the first harmonic components are mainly considered in this paper. In the figures, we can see that the simulated motions converge to the periodically steady state after 60 wave periods from the beginning of the simulation. Applying the Fourier analysis to the tail part of the time histories, $60 < t/T_w \leq 70$, the first harmonic components are obtained.

Fig.6(a) ~ 6(c) show the amplitude of floating body motions. Also in Fig.6, the linear theoretical value is drawn by the solid line and experimental data are plotted using black symbols. Agreement of simulation and linear theory is good for both $H_I = 1\text{cm}$ and 7cm . Near the resonant frequency of roll, simulated results for $H_I = 7\text{cm}$ are not plotted because the roll amplitude is so large that simulations diverge.

Fig.6(d) and 6(e) show the reflection and transmission coeffi-

cients of this radiation-diffraction problem. Also in these figures, the simulated values agree well with theoretical ones.

The wave drift force is plotted in Fig.6(f). Since the transmitted wave is very accurately simulated, the drift force computed from the transmitted wave agrees with the drift force using the linear theory. However, the pressure integral does not give an accurate drift force neither for the radiation-diffraction problem.

Wave amplitude dependency

The wave amplitude dependency on simulated motions, reflection and transmission coefficients and wave drift force are shown in Fig.7. Solid and broken lines are the values of linear theory for $\lambda = 2.094\text{m}$ and 1.571m , respectively. Since no clear wave amplitude dependency is perceived in the experimental data, only the simulated results are plotted in the figure using white symbols. The

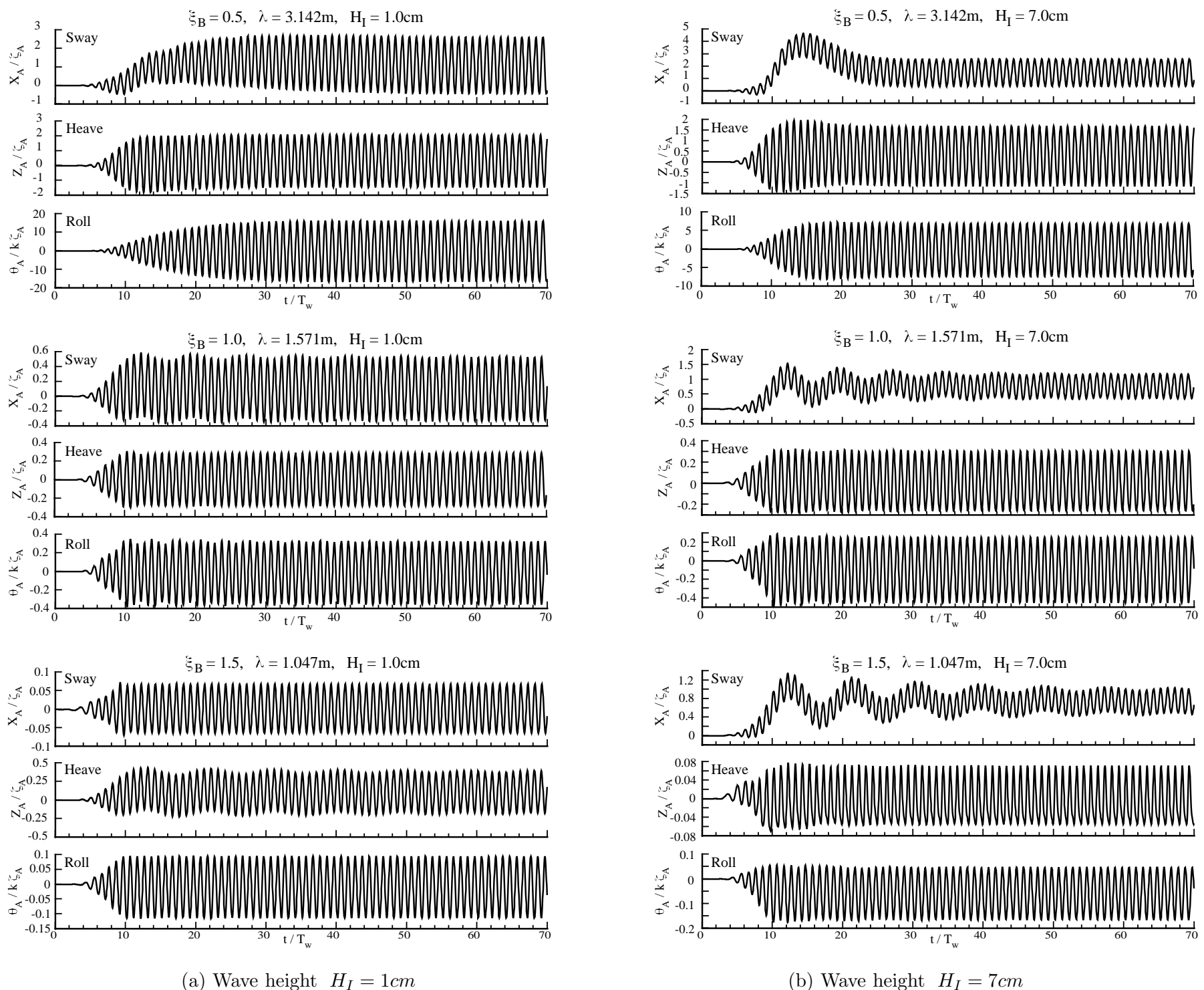


Fig.5: Simulated floating body motions

simulated drift force in Fig.7(f) is obtained from the transmission coefficient, which is considered to be accurate enough by the above accuracy confirmation. Simulated results for $\lambda = 1.571\text{m}$ have less amplitude dependency than those for $\lambda = 2.094\text{m}$. The frequency of the wave for $\lambda = 2.094\text{m}$ is nearer to the roll resonance frequency than that for $\lambda = 1.571\text{m}$. In case of $\lambda = 2.094\text{m}$, the roll motion has significant amplitude dependency and the other responses are considered to be affected by the roll motion; some of them have positive and others are negative wave amplitude dependency. The authors consider at present that the amplitude dependency is related to the roll resonance. Further study is required to obtain more convincing results.

CONCLUSIONS

A fully nonlinear numerical wave tank is applied to estimation of the wave drift force on two dimensional fixed and floating bodies. As the first step of this study, the accuracy of NWT is examined

and following results are obtained.

1. Simulated first harmonic wave exiting forces on fixed body agree well with theoretical values.
2. Simulated first harmonic floating body motions of a weakly moored floating body also agree well with theoretical values.
3. Simulated wave field around a body is also accurate and obtained reflection and transmission coefficients agree well with theoretical values.
4. Wave drift force obtained from simulated wave transmission coefficient agrees well with theoretical values.
5. Accuracy of the wave drift force obtained from direct pressure integral on the wetted body surface is not enough at the present stage.

For further study of the wave drift force, it is desirable that the pressure integral also gives accurate value. We are now seeking a reason of this discrepancy.

This study is a part of SRI's project research "On the drifting

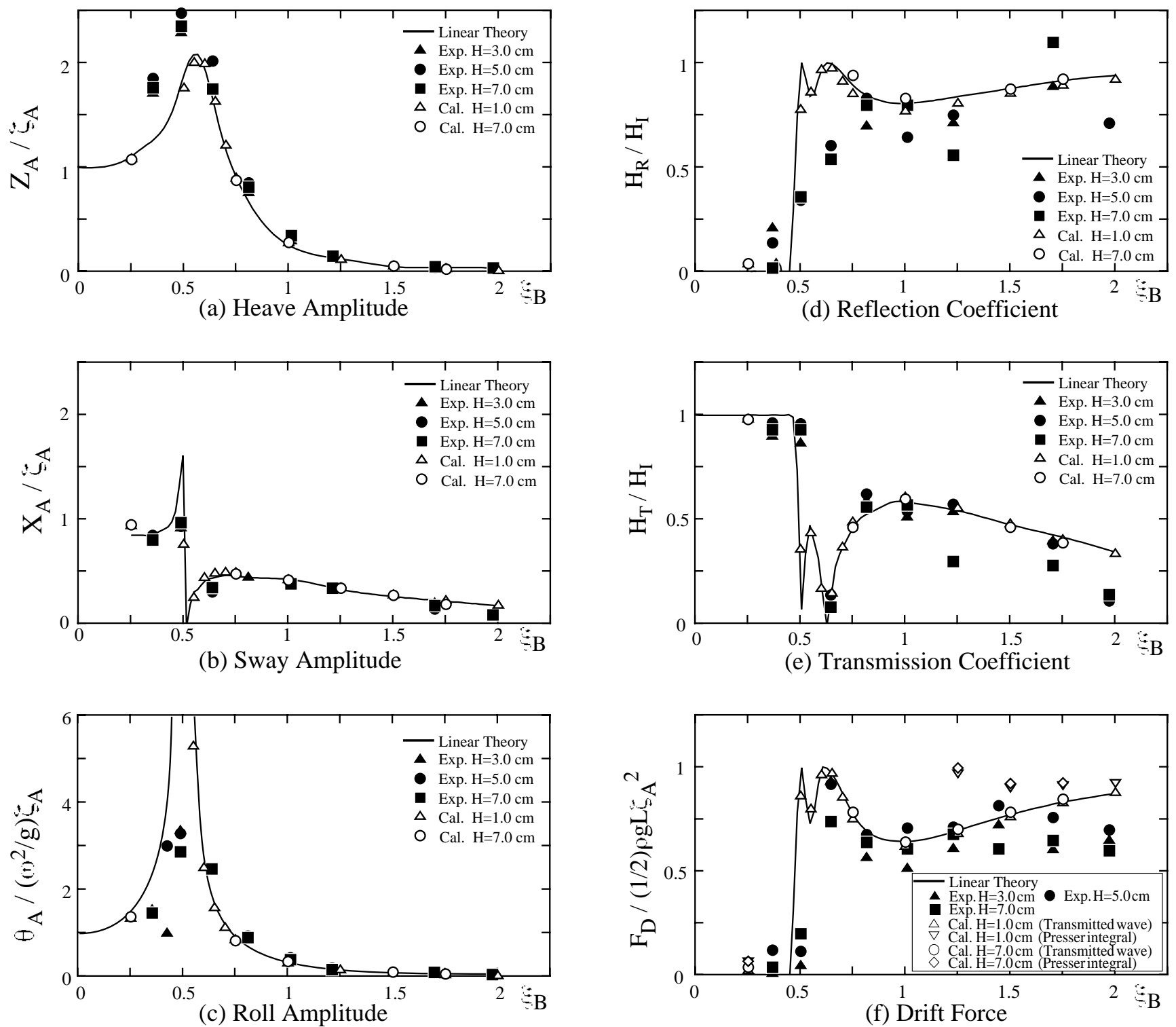


Fig.6: Simulated first harmonic component of the floating body motions, wave reflection and transmission coefficients and wave drift force.

prevention of disabled ships in rough waves” supported by the Ministry of Transport. Using NWT, effects of wave amplitude, water depth, and geometry of the sea bottom on the wave drift force will be studied.

REFERENCES

- 1) Maruo,H. (1960) “On the increase of the resistance of a ship in rough seas”, *J. Zosen Kiokai*, Vol.108
- 2) Nojiri,N. and Murayama,K. (1975) “A study on the drift force on two dimensional floating body in regular waves” *Trans. West-Japan Soc. Nav. Arch.*, Vol.51
- 3) Longuet-Higgins,M.S. and Cokelet,E. (1976), “The deformation of steep surface waves on water”, *Proc. Roy. Soc. ser.A350*, pp1-26
- 4) Goda,Y., Suzuki,Y.,Kishira,Y. and Kikuchi,O. (1976) “Estimation of incident and reflected waves in random wave experiments” *Rept. Port and Harbour Res. Inst.*, vol.248 ,pp3-24
- 5) Vinje, T. and Brevig, P. (1981), “Nonlinear Ship Motions”, *Proc. of the 3rd. Int. Conf. on Num. Ship Hydro.*, ppIV3-1-IV3-10
- 6) Cointe,R.,Geyer,P.,King,B.,Molin,B. and Tramoni,M. (1990), “Nonlinear and linear motions of a rectangular barge in perfect fluid”, *Proc. of the 18th Symp. on Naval Hydro.*, *Ann Arbor, Michigan*, pp85-98
- 7) Tanizawa, K. (1990), “A numerical method for nonlinear simulation of 2-D body motions in waves by means of B.E.M.”, *J. Soc. Nav. Arch. Japan*, Vol.168, pp223-228
- 8) Van Daalen, E.F.G. (1993), “Numerical and Theoretical Studies of Water Waves and Floating Bodies”, *Ph.D. thesis, University of Twente, The Netherlands*
- 9) Sen,D. (1993), “Numerical simulation of motions of two-dimensional floating bodies”, *Journal of Ship Research*, Vol.37, pp307-330

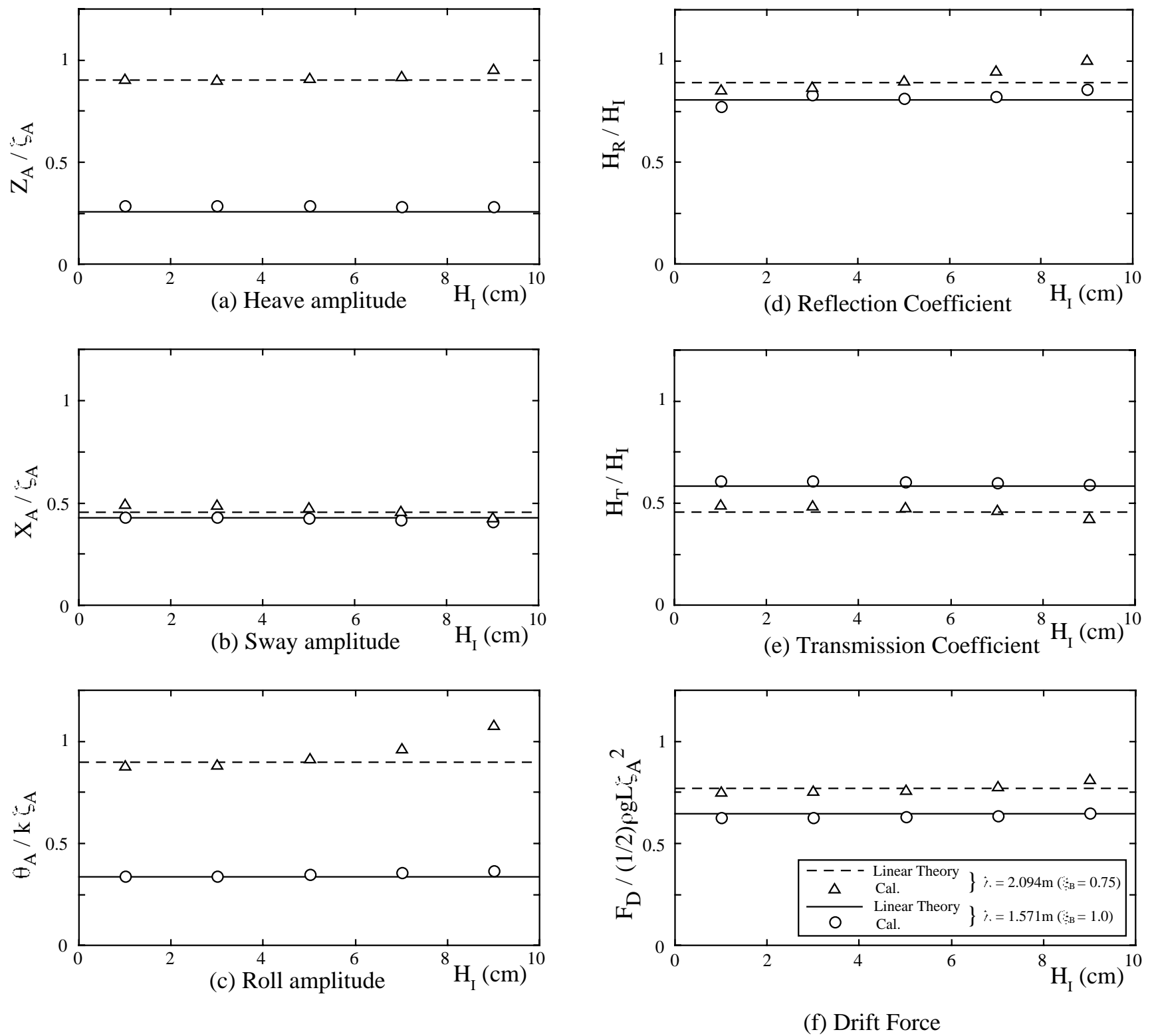


Fig.7: Wave amplitude dependency of the simulated first harmonic components and wave drift force.

- 10) Cao, Y., Beck, R. and Schultz, W.W. (1994), "Nonlinear motions of floating bodies in incident waves", *9th Workshop on Water Waves and Floating Bodies, Kuju, Oita*, pp33-37
- 11) Tanizawa, K. (1995) "A Nonlinear Simulation Method of 3-D Body Motions in Waves", *J. Soc. Nav. Arch. Japan*, Vol.178, pp179-191
- 12) Kashiwagi, M. (1996) "Full-nonlinear simulation of hydrodynamic forces on a Heaving two-dimensional body" *J. Soc. Nav. Arch. Japan*, Vol.180
- 13) Tanizawa, K. (1996) "Long time fully nonlinear simulation of floating body motions with artificial damping zone", *J. Soc. Nav. Arch. Japan*, Vol.180, pp311-319
- 14) Francescutto, A., Contento, G. and Armenio, V. (1996) "A fully hydrodynamic approach to the motion in waves of ships with free surface liquids on board" *11th Workshop on Water Waves and Floating Bodies, Hamburg*
- 15) Tanizawa, K. and Naito, S. (1997-1) "A study on parametric roll motions by fully nonlinear numerical wave tank", *Proc. of 11th ISOPE Conf., Honolulu, Hawaii*, Vol.3, pp69-75
- 16) Tanizawa, K. and Naito, S. (1997-2) "A study on wave drift damping by fully nonlinear simulation" *J. Kansai Soc. Nav. Arch. Japan*, Vol.228
- 17) Tanizawa, K. (1997-3) "Nonlinear theory of wave-body interaction based on acceleration potential and its application to numerical simulation" (in Japanese) *Ph.D thesis, Osaka Univ.*
- 18) Contento, G. (1997) "On the direct computation of large amplitude motions of floating bodies in regular and irregular waves", *Proc. of 6th STAB Conf., Varna, Bulgaria*, Vol.2, pp319-323
- 19) Tanizawa, K. (1998) "An application of fully nonlinear numerical wave tank to the study on chaotic roll motions" *Proc. of 8th ISOPE conference, Montreal, Canada*, Vol.3